J. Water Environ. Nanotechnol., 1(2): 124-134, Autumn 2016

ORIGINAL RESEARCH PAPER

Study of the Adsorption of Amido Black 10B Dye from Aqueous Solution Using Polyaniline Nano-adsorbent: Kinetic and Isotherm Studies

Marjan Tanzifi*, Mohsen Mansouri, Maryam Heidarzadeh, Kobra Gheibi

Department of Chemical Engineering, Faculty of Engineering, University of Ilam, Ilam, Iran

Received: 2016.08.27 Accepted: 2016.10.15 Published: 2016.11.01

ABSTRACT

In the present study, adsorptive properties of Polyaniline (PAn) were investigated for Amido Black 10B dye in aqueous solution. Different variables, including adsorption time, adsorbent dosage, solution pH and initial dye concentration were changed, and their effects on dye adsorption onto PAn nano-adsorbent were investigated. The study yielded the result that an increase in pH decreases the adsorption efficiency of nano-adsorbent. Also, Dye adsorption capacity increased with increase in the initial dye concentration. Optimum adsorption time and nano-adsorbent dosage were obtained 30 min and 0.1 gr, respectively. Kinetic studies illustrated that the Amido Black 10B dye adsorption process onto PAn nano-adsorbent followed the pseudo-second-order model, which indicates that the adsorption process is chemisorption-controlled. Also, adsorption equilibrium data were fitted to Freundlich isotherm. The maximum dye adsorption capacity, predicted by the Langmuir isotherm, was 142.85 mg/g. Moreover, Dubinin-Radushkevich isotherm showed that the adsorption of dye onto PAn nano-adsorbent is a chemisorption process.

KEYWORDS: *Amido Black 10B; Isotherm; Kinetic; Nano-adsorbent; Polyaniline*

How to cite this article

Tanzifi M, Mansouri M, Heidarzadeh M, Gheibi K, Study of the Adsorption of Amido Black 10B Dye from Aqueous Solution Using Polyaniline Nano-adsorbent: Kinetic and Isotherm Studies. J. Water Environ. Nanotechnol., 2016; 1(2):124-134. DOI: 10.7508/jwent.2016.02.006

INTRODUCTION

Dyes have been widely used for many years for various applications such as: textile, pigment, paint and etc. About 1.6 million tons of dyes are produced per year and 10–15% of this amount enters the wastewater stream [1,2]. Dyes are organic compounds containing one or more benzene rings. Such toxic materials cause irreparable damage to the environment and humans, such as cancer, mutagenesis, etc. Therefore, removal of dyes from water is essential and necessary [3]. Typically, dye is removed from water and wastewater using several methods such as electrochemical treatment [4], membrane filtration [5], photocatalytic degradation [6], as well as adsorption [7-9]. Adsorption technique is an appropriate and economic way to produce water with high quality. In adsorption process, elimination of pollutant from wastewater is conducted via binding it to an organic or inorganic adsorbent. The binding can be done by ion exchange, electrostatic, Vander Waals, etc. Dye adsorption process through adsorbent is dependent on various conditions such as adsorption time, pH of solution, particle size of adsorbent, temperature

* Corresponding Author Email: m.tanzifi@ilam.ac.ir

and presence of surfactants [10]. Application of nano-adsorbents in adsorption of contaminants from wastewater, due to their high specific surface area, high adsorption and desorption capacity and high reactivity, has received extensive consideration in recent years [11-13]. Different nano-adsorbents, including TiO_2/chitosan nanocomposite [14], flower-shaped Zinc oxide nanoparticles (ZON) [15], copper oxide nanoparticle loaded on activated carbon (Cu_2 O-NP-AC) [16], magnetic oxidized multiwalled carbon nanotube-k-carrageenan-Fe_3O_4 nanocomposite [17], graphene/Fe_3O_4/chitosan nanocomposite [18], have been used for removal of dye from wastewater.

Among the variety of industrial dyes, Amido Black 10B is a high toxicity dye which applied to both of natural and synthetics fibers namely, wool, cotton, silk, polyesters, rayon and acrylics. This diazo dye causes respiratory diseases and irritation of skin and eye [19]. Generally, a Little research has been done regarding the elimination of Amido Black 10B dye from wastewater by adsorption process. In the study conducted by Garg et al (2015), zeolite synthesized from fly ash was used as an adsorbent for the uptake of Amido Black 10B dye. It was found that optimum zeolite dosage and contact time were 10g/L and 6 hr, respectively. Also, maximum dye adsorption was obtained at low pH in the range 2-5 [19]. The results of the research carried out by Zhang et al (2016) showed that Zr (IV) surface-immobilized cross-linked chitosan/bentonite composite are highly efficient in removal of Amido Black 10B dye from aqueous solution. It was found that adsorption data fitted the Langmuir isotherm and the maximum adsorption capacity was reported to be 418.4 mg/g at natural solution pH (pH=6) and 298 K [20].

Polyaniline is one of the most important conductive polymers which has ion exchange properties and is capable of removing various contaminants such as heavy metals, nitrate, organic materials as well as dyes from water and wastewater. Various factors, including polymer synthesis conditions, the presence of surfactant, size of polymer and size and type of the dopant affect on ion exchange properties of polyaniline [21-23]. In the research carried out by Sharma et al (2016), polyaniline used for the adsorptive removal of cationic (crystal violet) and anionic (methyl orange) dyes from aqueous solutions. The adsorption capacity was obtained up to 245 and 220 mg/g for crystal violet and methyl orange, respectively. Furthermore, both dyes followed pseudo second order kinetic and Langmuir isotherm models [24]. Bhaumik etal (2013) showed that polypyrrole–polyaniline nanofibre is an effective adsorbent for removal of Congo red dye from aqueous solution. The maximum adsorption capacity was found to be 222.22 mg/g at 25 °C [25].

In the present work, the adsorption of Amido Black 10B dye from water using polyaniline nano-adsorbent is experimentally studied. The experiments were conducted to scrutinize the effect of different experimental parameters including pH of solution, nano-adsorbent dosage, initial concentration and adsorption time on adsorption efficiency of dye. Furthermore, kinetic and isotherm studies of Amido Black 10B adsorption on polyaniline nano-adsorbent were carried out.

EXPERIMENTAL

Materials and Instruments

Aniline monomer, ammonium peroxydisulfate, sulfuric acid, sodium hydroxide, sodium carboxymethyl cellulose and Amido Black 10B pigment were purchased from Merck (Germany). Aniline monomer was distilled once before polymerization to remove the impurities. The following instruments were also utilized in the process of the study: a magnetic stirrer (model HMS 8805, Iran), digital scale (model Traveler TA30), scanning electron microscope (SEM) (model KYKY-EM3200, China) and Fourier-transform infrared (FTIR) spectrometer (model VERTEX 70; Bruker, Germany). Moreover, UV–visible spectroscopy (UV-VIS) (model Perkin Elmer, lambda 25) was used to determine the concentration of dye in the solution. The spectroscopy was calibrated using standard Amido Black 10B solutions (0.25-15 ppm).

Synthesis of Nano-adsorbent

In order to prepare PAn nano-adsorbent, 2.5 g of ammonium peroxydisulfate as oxidizing agent, was added to 100 ml of 1M sulfuric acid containing sodium carboxymethyl cellulose (0.1 g) as a surfactant. The solution was stirred by a magnetic stirrer for 30 minutes. Afterwards, 1 ml of aniline monomer was added drop-wise to the solution. The solution was filtered after 5 hr. In order to remove

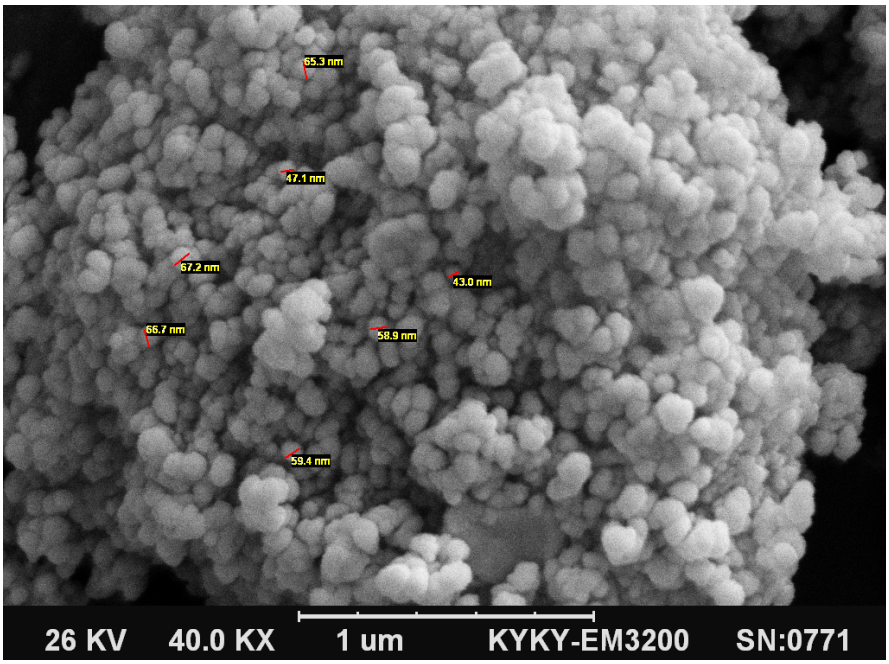

Fig. 1. Scanning electron microscopy of Polyaniline nano-adsorbent

oligomers, impurities and acid, the polymer was washed several times with distilled water. The final product was dried for 48 hours in an oven at 45 °C and converted into a fine powder.

Dye Adsorption Experiments

Different parameters including adsorbent dosage, pH, adsorption time and initial dye concentration were changed, and their impacts on the efficiency of PAn nano-adsorbent in removing Amido Black 10B dye from solution was investigated. Also, kinetic and isotherm studies of dye adsorption were carried out. In all experiments, solution volume and stirring speed were 50 ml and 500 rpm. Sulfuric acid and sodium hydroxide were used to change the pH of solution. A specified amount of nano-adsorbent was added to the initial solution with certain dye concentration. The solution was next stirred using a magnetic stirrer for a certain time. Afterwards, it was filtered, and the concentration of dye in solution was determined using a UV-Vis spectrophotometer at 618 nm maximum wavelength.

Removal efficiency of dye was determined using the following equation:

$$(\%) = \frac{C_i - C_f}{C_i} \times 100 \quad (1)$$

Where, C_i (mg/l) and C_f (mg/l) are the initial and final dye concentrations, respectively. q_t (mg/g) is dye adsorption capacity at time (t), and q_e (mg/g) is the amount of adsorption at equilibrium, which were calculated as follows:

$$q_t = (C_i - C_t) \times \frac{V}{m} \quad (2)$$

$$q_e = (C_i - C_e) \times \frac{V}{m} \quad (3)$$

Where, C_t is the concentration of dye at time (t); C_e is the equilibrium concentration of dye; V is the solution volume (ml) and m is the PAn nano-adsorbent mass (gr).

RESULTS AND DISCUSSION

Characterization of Nano-adsorbent

The morphology of the synthesized nano-adsorbent was investigated using scanning electron microscopy (SEM). Fig. 1 shows the SEM image of PAn nano-adsorbent. As shown in figure, the synthesized adsorbent particles feature nano-scaled size (The average size is about 59 nm), uniform distribution, and spherical shape. Presence of surfactant in polymer synthesis environment, lead to a decrease in particle size. surfactant can either form a chemical bond with polymer or be physically adsorbed, consequently preventing the excessive growth of the polymer chain and accumulated mass of particles during polymerization. Nano-adsorbent has high specific surface area and consequently

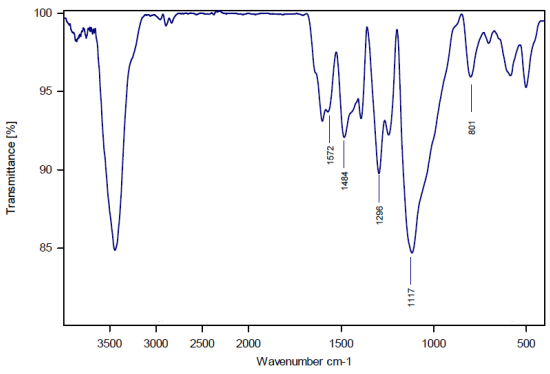

Fig. 2. Fourier Transform Infrared Spectroscopy of Polyaniline nano-adsorbent

high adsorption capacity.

Fig. 2 shows the infrared spectrum of PAn nano-adsorbent within the range of 450-4000 Cm^{-1}. As can be seen, the FTIR spectrum of nano-adsorbent features peaks at wavelength 1572, 1484, 1296, 1117, 801 Cm^{-1} ascribed to (C=C stretching vibration of the quinoid ring), (C=C stretching vibration of the benzenoid ring), (C-N stretching vibration), (C-H in-plane deformation), and (C-H out-of-plane deformation), respectively [26].

Effect of pH

The pH of solution is one of the main factors affecting the adsorption of adsorbate since adsorbent surface charge and the degree of ionization of adsorbate are influenced by pH. For investigation the effect of PH of solution on adsorption efficiency, the range of pH was considered to be 2-10. Adsorbent dosage, initial concentration and volume of dye solution were 0.1 gr, 30mg/l and 50 ml, respectively. The result was illustrated in Fig. 3. As it is shown in the figure, adsorption efficiency decreases with increase in pH value of solution. An increase in the pH of solution leads to an increase in the negative charge density of the adsorbent surface area. The electrostatic repulsion between the negatively charged pigment and negatively charged surface of the adsorbent reduces dye adsorption. However, decreasing the pH of solution increases the adsorption efficiency of nano-adsorbent. The reason might lie in the fact that at low pH, active sites in the structure of nano-adsorbent can be protonated. As a result, the positive charge density of adsorbent surface area increases, and consequently, dye adsorption efficiency increases due to electrostatic attraction.

More dye adsorption happened at pH values lower than 6. Hence, the optimum pH of Amido Black 10B dye solution is in the range 2–6. Therefore, the pH of 6 (natural solution pH) was used for all other experiments.

Effect of Nano-adsorbent Dosage

Adsorbent dosage is one of the effective parameters in determining dye adsorption efficiency. Gaining higher adsorption efficiency with less adsorbent dosage reduces the adsorption cost. In order to evaluate the effect of nano-adsorbent dosage on dye adsorption, different amounts of PAn (0.02-0.2 gr) was added to 50 ml of 30 mg/l dye solution. The effect of nano-adsorbent dosage on dye adsorption efficiency is shown in Fig. 4. As can be seen, an increase in nano-adsorbent dosage leads to a rise in adsorption efficiency. Dye adsorption efficiency per 0.1 g of nano-adsorbent dosage was measured 95%, and then remains constant in the range of 0.1-0.2 gr. Therefore, the optimum nano-adsorbent dosage was considered to be 0.1 g.

Effect of Adsorption Time and Dye Adsorption Kinetics

Fig. 5 illustrates the effect of adsorption time on dye adsorption efficiency. The effect of adsorption time on dye adsorption efficiency, was done with the change in time from 1 to 60 min. As can be seen, increasing the adsorption time from 1 min to 30 min causes the adsorption efficiency to increase and remain constant afterwards. As a result, the optimum adsorption time of PAn nano-adsorbent was determined to be 30 min.

The results of the change of adsorption time were analyzed to obtain information about the kinetics of adsorption onto PAn nano-adsorbent. The adsorption kinetics of Amido Black 10B dye onto PAn nano-adsorbent was investigated using the three equations: pseudo-first-order, pseudo-second-order, and Weber–Morris.

Pseudo-first-order kinetic model is based on the assumption that the process of adsorption can be controlled by weak interaction between adsorbate and adsorbent surface (physical adsorption). Linear form of pseudo-first-order equation [27] is expressed as follows:

$$log(q_e - q_t) = logq_e - \left(\frac{K_1}{2.303}\right)t \quad (4)$$

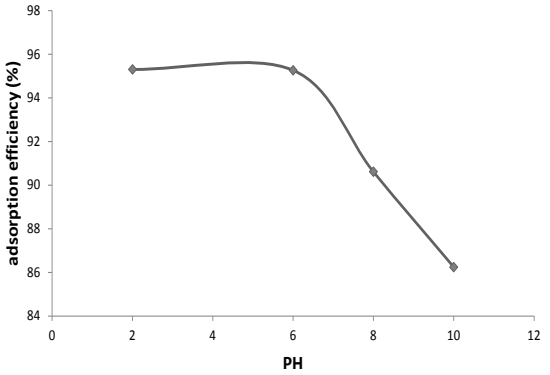

Fig. 3. Effect of pH on adsorption efficiency of Amido Black 10B dye onto Polyaniline nano-adsorbent

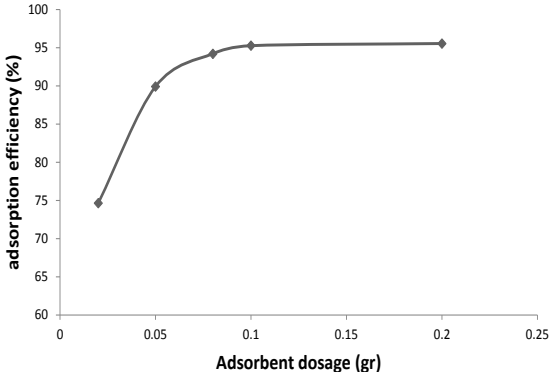

Fig. 4. Effect of adsorbent dosage on adsorption efficiency of Amido Black 10B dye onto Polyaniline nano-adsorbent

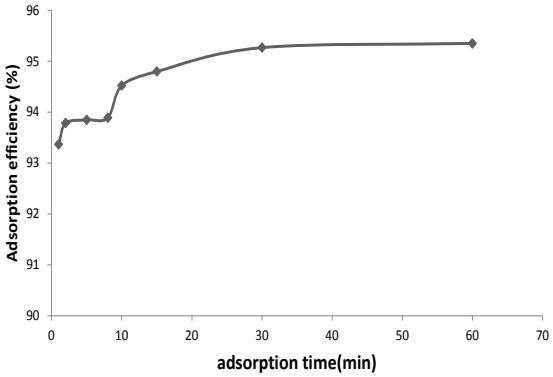

Fig. 5. Effect of adsorption time on adsorption efficiency of Amido Black 10B dye onto Polyaniline nano-adsorbent

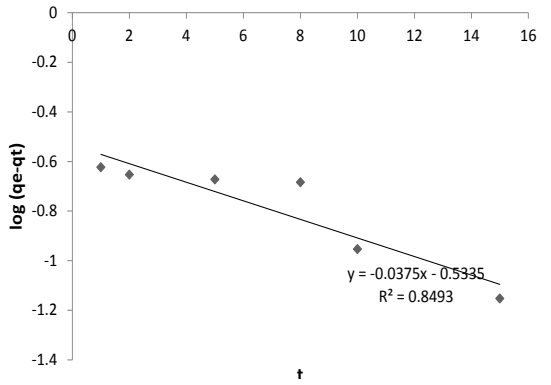

Fig. 6. Pseudo-first-order plot of Amido Black 10B adsorption onto Polyaniline nano-adsorbent

Where q_e (mg/g) and q_t (mg/g) are the amount of dye adsorbed at equilibrium and at time (t); and K_1 is the rate constant of pseudo-first-order equation. Fig. 6 shows the plot of the pseudo-first-order model for dye adsorption on PAn nano-adsorbent. The correlation coefficient and rate constant of the pseudo-first-order model were presented in Table 1.

The adsorption kinetic of Amido Black 10B dye was also investigated using pseudo-second-order model. This kinetic model assumes that the process of dye adsorption is chemisorption. This model is expressed as follows [28]:

$$q_t = \frac{K_2 {q_e}^2 t}{1+K_2 q_e t} \quad (5)$$

Where, K_2 is the rate constant of pseudo-second-order model. This equation is presented in four linear forms, i.e. type 1, type 2, type 3, and type 4 which were shown in Table 1. Moreover, the plots of pseudo-second-order model for dye adsorption through PAn nano-adsorbent were presented in Figs. 7a-7d. As the figures show, the pseudo-second-order model, type 1 results in a better correlation coefficient in comparison to the other types of pseudo-second-order model.

In order to determine whether intraparticle diffusion is a rate-controlling step in dye adsorption, Weber-Morris model was used for the analysis of the kinetic data. The Weber-Morris model can be written as follows [29]:

$$q_t = K_{id}(t)^{0.5} + C \quad (6)$$

Where, K_{id} is rate constant of Weber-Morris model; and C is a constant that gives an idea about the thickness of the boundary layer. If the plot q_t versus $t^{0.5}$ is linear, the process of dye adsorption is controlled by diffusion resistance. When the plot passes through the origin, it indicates that intraparticle diffusion is the only rate-controlling step. The slope and intercept of the plot (Fig. 8) can be used to calculate values for the constants K_{id} and C, respectively. The values were presented in Table 1.

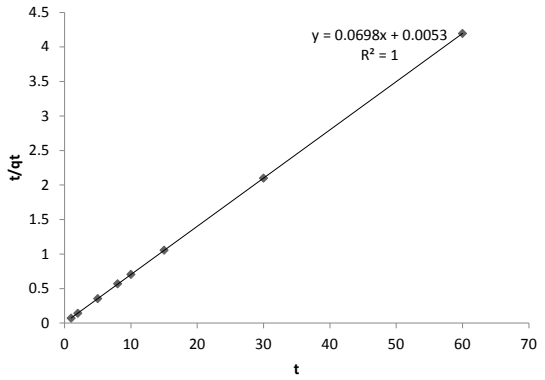

Fig. 7(a). Pseudo-second-order plot of Amido Black 10B adsorption onto Polyaniline nano-adsorbent (type 1)

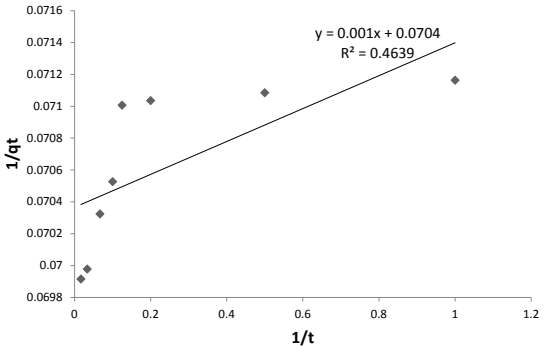

Fig. 7(b). Pseudo-second-order plot of Amido Black 10B adsorption onto Polyaniline nano-adsorbent (type 2)

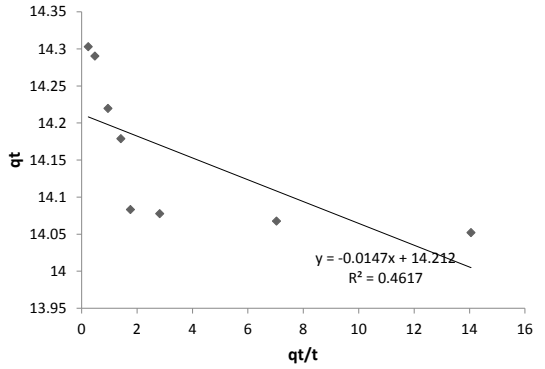

Fig. 7(c). Pseudo-second-order plot of Amido Black 10B adsorption onto Polyaniline nano-adsorbent (type 3)

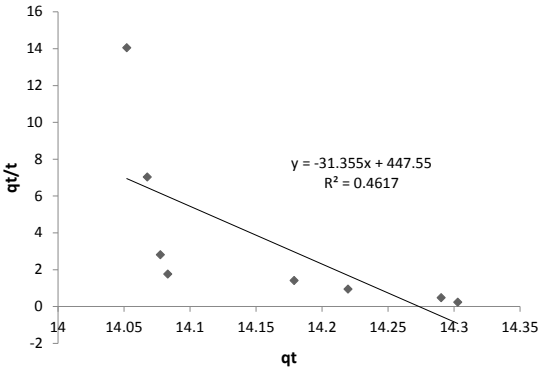

Fig. 7(d). Pseudo-second-order plot of Amido Black 10B adsorption onto Polyaniline nano-adsorbent (type 4)

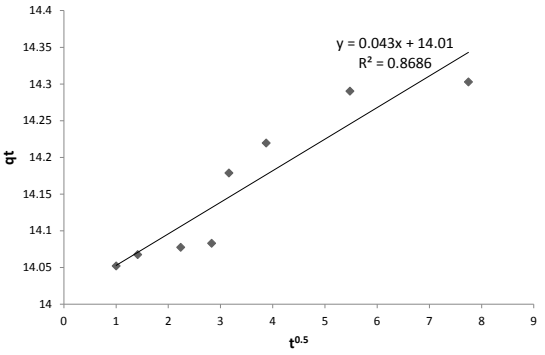

Fig. 8. Weber-Morris plot of Amido Black 10B adsorption onto Polyaniline nano-adsorbent

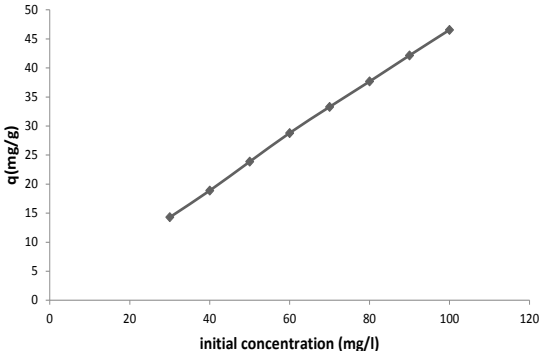

Fig. 9. Effect of initial concentration on adsorption capacity of Amido Black 10B dye onto Polyaniline nano-adsorbent

The correlation coefficient *(R^2)* of the three kinetic models, i.e. pseudo-first-order, pseudo-second-order (type 1), and Weber–Morris equations for dye adsorption on PAn nano-adsorbent was obtained as 0.8493, 1, and 0.8686, respectively (Table 1). So, the experimental data were well described by the pseudo-second-order kinetic model, which indicates that the process of Amido Black 10B dye adsorption onto PAn nano-adsorbent is chemisorption-controlled. Also, dye adsorption capacity obtained through pseudo-second-order kinetic model was very close to its experimental value.

Table 1. Kinetic constants for Amido Black 10B dye adsorption

Kinetic model	Parameters	R^2
Pseudo-first-order	$q_e(Experimental) = 14.29$ $q_e = 0.2927$, $K_1 = 0.00863$	0.8493
Pseudo-second-order	$q_e(Experimental) = 14.29$	
Type 1: $\frac{t}{qt} = \frac{1}{K_2 qe^2} + \frac{1}{qe}t$	$q_e = 14.32$, $K_2 = 0.9192$	1
Type 2: $\frac{1}{qt} = \frac{1}{qe} + \frac{1}{K_2 qe^2}\left(\frac{1}{t}\right)$	$q_e = 14.20$, $K_2 = 4.9561$	0.4639
Type 3: $qt = qe - \frac{1}{K_2 qe}\left(\frac{qt}{t}\right)$	$q_e = 14.21$, $K_2 = 4.7866$	0.4617
Type 4: $\frac{qt}{t} = K_2 qe^2 - K_2(qe)qt$	$q_e = 14.27$, $K_2 = 2.1969$	0.4617
Weber-Morris	$C = 14.01$, $K_{id} = 0.043$	0.8686

Table 2. Isotherm constants for Amido Black 10B dye adsorption

Isotherm model	Parameters	R^2
Freundlich	$n = 0.79157$, $K_F = 0.04794$	0.9579
Langmuir		
Type 1: $\frac{C_e}{q_e} = \frac{1}{K_L q_m} + \frac{1}{q_m}C_e$	$q_m = 102.04$, $K_L = 0.1259$, $R_L = 0.07358 - 0.20933$	0.7478
Type 2: $\frac{1}{q_e} = \frac{1}{q_m K_L C_e} + \frac{1}{q_m}$	$q_m = 142.85$, $K_L = 0.0810$, $R_L = 0.10989 - 0.29154$	0.9243
Type 3: $q_e = q_m - \frac{q_e}{K_L C_e}$	$q_m = 66.837$, $K_L = 0.2525$, $R_L = 0.03809 - 0.11661$	0.3731
Type 4: $\frac{q_e}{C_e} = K_L q_m - K_L q_e$	$q_m = 127.61$, $K_L = 0.0942$, $R_L = 0.09597 - 0.26137$	0.3731
Temkin	$B = 20.483$, $K_T = 0.33786$	0.9574
Dubinin–Radushkevick	$\beta = 6 \times 10^{-9}$, $X_m = 103.87$, $E = 9.12$	0.8474

Effect of Initial Concentration and Dye Adsorption Isotherm

In order to investigate the effect of initial concentration on adsorption capacity, Amido Black 10B dye solutions with the initial concentration of 30-100 mg/l were prepared. Fig. 9 shows the plot of the adsorption capacity based on the initial concentration of dye. As can be seen, the adsorption capacity of nano-adsorbent increased with increasing the initial concentration. When the initial concentration of the solution changed from 30 mg/l to 100 mg/l, the adsorption capacity of PAn nano-adsorbent increased from 14.29 to 46.55 mg/g.

The relationship between dye concentration in solution and the amount of dye adsorbed on the solid phase at equilibrium was described by isotherm models. In this study, four adsorption isotherm models namely Langmuir, Freundlich, Temkin, and Dubinin–Radushkevich were applied to explain adsorption isotherm of Amido Black 10B dye onto PAn nano-adsorbent.

Langmuir isotherm model assumes adsorption energy is independent of surface coverage and adsorption is limited to a monolayer. Langmuir isotherm model is expressed as follows [30]:

$$q_e = \frac{q_m K_L C_e}{1 + K_L C_e} \quad (7)$$

Here, q_m is the maximum adsorption capacity (mg/g); and K_L is adsorption constant of Langmuir

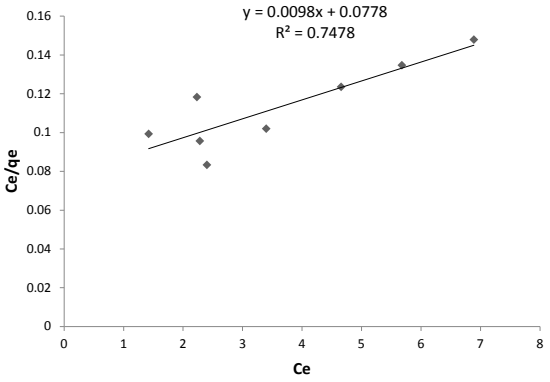

Fig. 10 (a). Langmuir adsorption isotherm of Amido Black 10B onto Polyaniline nano-adsorbent (type 1)

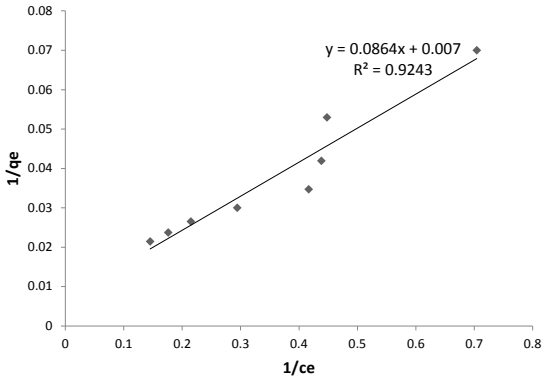

Fig. 10 (b). Langmuir adsorption isotherm of Amido Black 10B onto Polyaniline nano-adsorbent (type 2)

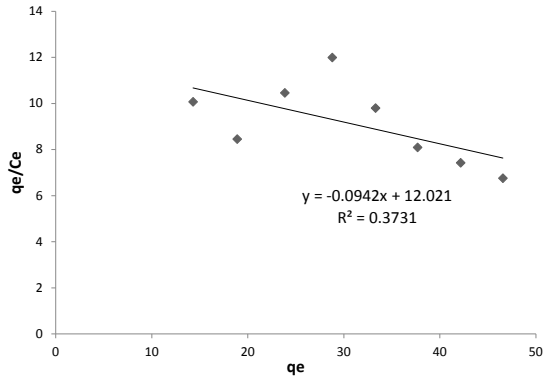

Fig. 10 (c). Langmuir adsorption isotherm of Amido Black 10B onto Polyaniline nano-adsorbent (type 3)

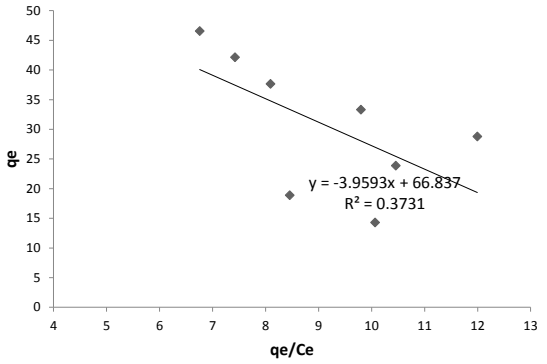

Fig. 10 (d). Langmuir adsorption isotherm of Amido Black 10B onto Polyaniline nano-adsorbent (type 4)

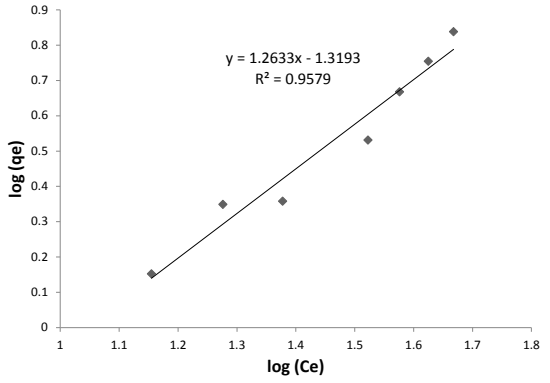

Fig. 11. Freundlich adsorption isotherm of Amido Black 10B onto Polyaniline nano-adsorbent

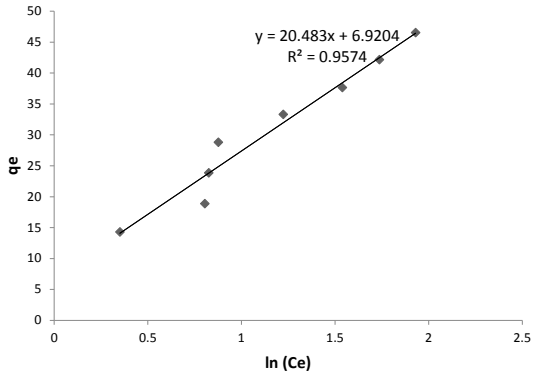

Fig. 12. Temkin adsorption isotherm of Amido Black 10B onto Polyaniline nano-adsorbent

isotherm. Langmuir isotherm can be linearized into four different types, as displayed in Table 2. The value of maximum adsorption capacity and constant of Langmuir isotherm were calculated from intercept and slope of Linear Langmuir plots (Figs. 10a-10d). As the figures show, Linear Langmuir equations, type 2 has a higher correlation coefficient in comparison to the other linear equations. Separation factor (R_L) is a dimensionless constant which expresses the essential features of the Langmuir isotherm [31]:

$$R_L = \frac{1}{1+K_L c_i} \quad (8)$$

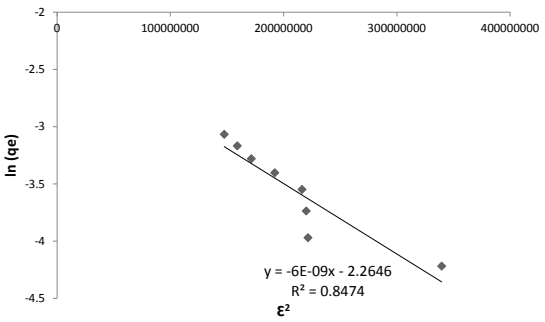

Fig. 13. D-R adsorption isotherm of Amido Black 10B onto Polyaniline nano-adsorbent

In this equation, C_i is the initial concentration of dye; and K_L is constant of Langmuir isotherm. Dye adsorption process onto PAn nano-adsorbent is favorable when the value of R_L obtained in the range 0-1. The separation factors from Linear Langmuir equation (type 2) obtained in the range of 0.10989-0.29154.

The Freundlich isotherm is an empirical model based on the adsorption on heterogeneous surface. This model does not predict the maximum adsorption. Also it is suitable for multilayer adsorption. The Freundlich equation is described as follows [32]:

$$q_e = K_F(C_e)^{1/n} \quad (9)$$

Where, K_F and 1/n are Freundlich constant and adsorption intensity, respectively. Freundlich equation can be linearized as follows:

$$log(q_e) = log(K_F) + \frac{1}{n} log(c_e) \quad (10)$$

Freundlich constants (K_F) and n were calculated from the intercept and the slope of the linearized plots of $log(q_e)$ versus $log(c_e)$ The plot of Freundlich model was presented in Fig. 11.

Temkin Isotherm contains a factor that represents interaction between nano-adsorbent and dye. The linear form of Temkin isotherm is expressed as follows [33]:

$$q_e = B\ln(K_T) + Bln\,(C_e) \quad , \quad B = \frac{RT}{bT} \quad (11)$$

Where, K_T is equilibrium binding constant of Temkin isotherm(L/g); b_T is constant of Temkin isotherm; R is the universal gas constant (8.314 J/mol.K); T is temperature in Kelvin(293.15 K); and B is constant related to the adsorption heat(J/mol). Values of B and K_T can be obtained via plot of q_e versus $ln(C_e)$ (Fig. 12), which were represented in Table 2.

Dubinin–Radushkevich isotherm [34] is used to investigate the type of Amido Black 10B dye adsorption on PAn nano-adsorbent (physical or chemical). The linear form of D-R model is presented in the following equation:

$$\ln(q_e) = ln(X_m) - \beta\varepsilon^2 \quad where \quad \varepsilon = \mathrm{RT}\ln(1+\frac{1}{C_e}) \quad (12)$$

In these equations, C_e, e, X_m and b are the dye equilibrium concentration, polanyi potential, maximum adsorption capacity and constant related to the adsorption energy, respectively. The value of b calculated from the slope of $Ln(q_e)$ versus ε^2 plot (Fig 13). The average adsorption energy, E (kJ/mol), obtained by b is calculated by the following equation:

$$E = (2\beta)^{-0.5} \quad (13)$$

If the value of E is between 8 and 16 kJ/mol, the adsorption process is chemisorption whereas if E<8 kJ/mol, the adsorption process is of physical nature. The results of the study indicated that the process of Amido Black 10B dye adsorption onto PAn nano-adsorbent is chemisorption.

As shown in Table 2, Freundlich adsorption isotherm shows the best fit to Amido Black 10B dye adsorption data on PAn nano-adsorbent because this model has a higher correlation coefficient (R^2= 0.9579).

CONCLUSION

PAn nano-adsorbent was prepared through chemical polymerization and used as an adsorbent of Amido Black 10B dye from aqueous solution. SEM and FTIR were used to examine the morphology and chemical structure of the synthesized nano-adsorbent. The results of SEM indicated that the synthesized adsorbent particles feature nano-scaled size, uniform distribution, and spherical shape. Such characteristics have been attributed to high efficiency adsorbents. Moreover, FTIR spectrum has proved the formation of PAn nano-adsorbent. The adsorption experiments indicated that PAn nano-adsorbent has high efficiency in Amido Black 10B dye adsorption. The research also yielded the result that optimum adsorption time and adsorbent dosage of PAn nano-adsorbent was 30 min and 0.1 gr, respectively. Dye adsorption was influenced by pH of solution, that is, adsorption efficiency decreases by increasing of pH. Also, dye adsorption

capacity increased with increase in the initial dye concentration. The kinetic data illustrated that the adsorption process was controlled by pseudo-second-order model, which indicates that the dye adsorption is chemisorption in nature. Also, the adsorption capacity which calculated by this model (type 1) was 14.32 mg/g, which is close to the experimental value (14.29 mg/g). The results of isotherm studies revealed that the experimental data were best represented by Freundlich isotherm model. The correlation coefficient of this model was obtained 0.9579. The maximum adsorption capacity obtained from Langmuir model, was 142.85 mg/g. The separation factors were in the range of 0-1, indicating that the adsorption of Amido Black 10B dye onto PAn nano-adsorbent was favorable. Moreover, the results obtained from D-R Isotherm showed that the process of dye adsorption onto PAn nano-adsorbent was chemical adsorption. The average adsorption energy was obtained 9.12 KJ/mol.

CONFLICT OF INTEREST

The authors declare that there are no conflicts of interest regarding the publication of this manuscript.

REFERENCES

1. Liu, J., D. Guo, Y. Zhou, Z. Wu, W. Li, F. Zhao and X. Zheng, 2011. Identification of ancient textiles from Yingpan, Xinjiang, by multiple analytical techniques. Journal of Archaeological Science. 38 (7): 1763–1770.
2. Hunger, K., 2003. Industrial Dyes-Chemistry, Properties, Application, Wiley.
3. Daneshvar, N., D. Salari and A.R., Khataee, 2003. Photocatalytic degradation of azo dye acid red 14 in water: investigation of the effect of operational parameters. Journal of Photochemistry and Photobiology A: Chemistry, 157 (1): 111-116.
4. Elaissaoui, I., H. Akrout, S. Grassini, D. Fulginiti and L. Bousselmi, 2016. Role of SiO_x interlayer in the electrochemical degradation of Amaranth dye using SS/PbO_2 anodes. Materials and Design, 110: 633–643.
5. Alventosa-deLara, E., S. Barredo-Damas, M.I. Alcaina-Miranda and M.I. Iborra-Clar, 2012. Ultrafiltration technology with a ceramic membrane for reactive dye removal: optimization of membrane performance, Journal of Hazardous Materials. 209–210: 492–500.
6. Sabbaghi. S. and F. Doraghi, 2016. Photo-Catalytic degradation of Methylene blue by ZnO/SnO_2 nanocomposite. Journal of water and environmental nanotechnology, 1 (1): 27-34.
7. Lin, Y.F. and F.L. Liang, 2016. ZrO_2/carbon aerogel composites: A study on the effect of the crystal ZrO_2 structure on cationic dye adsorption. Journal of the Taiwan Institute of Chemical Engineers, 65: 78–82.
8. Liu, K., L. Chen, L. Huang and Y. Lai, 2016. Evaluation of ethylenediamine-modified nanofibrillated cellulose/chitosan composites on adsorption of cationic and anionic dyes from aqueous solution. Carbohydrate Polymers, 151: 1115–1119.
9. Liu, F., Z. Guo, H. Ling, Z.H. Huang and D. Tang, 2016. Effect of pore structure on the adsorption of aqueous dyes to ordered mesoporous carbons. Microporous and Mesoporous Materials, 227: 104–111.
10. Ramalho, P.A., M.C. Roberto and A.P. Cavaco, 2005. Degradation of dyes with mocroorganisms: studies with ascomycete yeasts. Universidade Do Minho.
11. Tian, J., J. Xu, F. Zhu, T. Lu, C. Su and G. Ouyang, 2013. Application of nanomaterials in sample preparation. Journal of Chromatography A., 1300: 2-16.
12. Rahmanzadeh, L. M. Ghorbani and M. Jahanshahi, 2016. Effective removal of hexavalent mercury from aqueous solution by modified polymeric nanoadsorbent. Journal of water and environmental nanotechnology, 1 (1): 1-8.
13. Samadi, S., R. Motallebi and M. Nasiri Nasrabadi, 2016. Synthesis, characterization and application of Lanthanide metal-ion-doped TiO_2/bentonite nanocomposite for removal of Lead (II) and Cadmium (II) from aquatic media. Journal of water and environmental nanotechnology, 1 (1): 35-44.
14. Kamal , T., Y. Anwar, S.H. Bahadar Khan, M.T. Saeed Chani and A.M. Asiri, 2016. Dye adsorption and bactericidal properties of TiO_2/chitosan coating layer. Carbohydrate Polymers, 148: 153–160
15. Kataria, N., V.K. Garg, M. Jain and K. Kadirvelu, 2016. Preparation, characterization and potential use of flower shaped Zinc oxide nanoparticles (ZON) for the adsorption of Victoria Blue B dye from aqueous solution. Advanced Powder Technology, 27 (4): 1180–1188.
16. Agarwal, S., I. Tyagi, V.K. Gupta , A.R. Bagheri, M. Ghaedi , A. Asfaram, S. Hajati and A.A. Bazrafshan, 2016. Rapid adsorption of ternary dye pollutants onto copper (I) oxide nanoparticle loaded on activated carbon: Experimental optimization via response surface methodology. Journal of Environmental Chemical Engineering, 4 (2): 1769–1779.
17. Duman , O., S. Tunç , T. Gürkan Polat, B. Kancı Bozoğlan, 2016. Synthesis of magnetic oxidized multiwalled carbon nanotube-κ-carrageenan-Fe_3O_4 nanocomposite adsorbent and its application in cationic Methylene Blue dye adsorption. Carbohydrate Polymers, 147: 79–88.
18. Van Hoa , N., T.H. Trung Khong, T.T. Hoang Quyen and T.S. Trung, 2016. One-step facile synthesis of mesoporous graphene/Fe_3O_4/chitosan nanocomposite and its adsorption capacity for a textile dye. Journal of Water Process Engineering, 9: 170–178.
19. Garg, A., M. mainrai, V. kumar bulasara and S. barman, 2015. Experimental Investigation on Adsorption of Amido Black 10B Dye onto Zeolite Synthesized from Fly Ash. Chemical Engineering Communications, 202 (1):123–130.
20. Zhang, L., P. Hu, J. Wang and R. Huang, 2016. Adsorption of Amido Black 10B from aqueous solutions onto Zr (IV) surface-immobilized cross-linked chitosan/bentonite composite. Applied Surface Science, 369: 558–566.
21. Weidlich, C., K.M. Mangold and K. Juttner, 2001. Conducting polymers as ion-exchangers for water purification. Electrochimica Acta, 47 (5): 741–745.
22. Zhou, Q., Y. Wang, J. Xiao, H. Fan, 2016. Adsorption and removal of bisphenol A, α-naphthol and β-naphthol from aqueous solution by Fe_3O_4@polyaniline core–shell nanomaterials. Synthetic Metals, 212: 113–122.
23. Hojjat Ansari, M. and J. Basiri Parsa, 2016. Removal of nitrate from water by conducting polyaniline via electrically

switching ion exchange method in a dual cell reactor: Optimizing and modeling. Separation and Purification Technology, 169: 158–170.
24. Sharma, V., P. Rekha and P. Mohanty, 2016. Nanoporous hypercrosslinked polyaniline: An efficient adsorbent for the adsorptive removal of cationic and anionic dyes. Journal of Molecular Liquids, 222: 1091–1100.
25. Bhaumik, M., R. McCrindle and A. Maity. 2013. Efficient removal of Congo red from aqueous solutions by adsorption onto interconnected polypyrrole–polyaniline nanofibres. Chemical Engineering Journal, 228: 506–515.
26. Ghorbani, M., M. Soleimani Lashkenari and H. Eisazadeh, 2011. Application of polyaniline nanocomposite coated on rice husk ash for removal of Hg(II) from aqueous media. Synthetic Metals, 161: 1430– 1433.
27. Lagergren, S., 1898. About the theory of so-called adsorption of soluble substances. _handlingar, 24 (4): 1-39.
28. Ho, Y.S. and G. McKay, 1999. Pseudo-second order model for sorption processes. Process Biochemistry, 34 (5): 451–465.
29. Weber, W.J. and J.C. Morris, 1963. Kinetics of Adsorption on Carbon from Solution. Journal of the Sanitary Engineering Division, 89 (2): 31-60.
30. Langmuir, I., 1916. The Constitution and Fundamental Properties of Solids and Liquids. Part1. Solids. Journal of the American chemical Society, 38 (11): 2221-2295.
31. Weber, T.W. and R.K. Chakraborti, 1974. Pore and solid diffusion models for fixed bed adsorbents. AIChE Journal, 20 (2): 228–238.
32. Freundlich, H.M.F., 1906. Uber die adsorption in losungen. Zeitschrift fur Physikalische Chemie-Leipzig., 57 (A): 385-470.
33. Tempkin, M.J. and V. Pyzhev, 1940. Kinetics of Ammonia Synthesis on Promoted Iron Catalysts. Acta Physicochimica URSS, 12: 217-222.
34. Dubinin M.M. and L.V. Radushkevich, 1947. The equation of the characteristic curve of activated charcoal. Physical Chemistry Section, U.S.S.R., 55: 331-337.